Eur. Phys. J. A **25**, s01, 363–366 (2005)
DOI: 10.1140/epjad/i2005-06-016-2

EPJ A direct
electronic only

News on mirror nuclei in the sd and fp shells

J. Ekman[a], L.-L. Andersson, C. Fahlander, E.K. Johansson, R. du Rietz, and D. Rudolph

Department of Physics, Lund University, S-22100 Lund, Sweden

Received: 3 December 2004 /
Published online: 3 May 2005 –

Abstract. Novel experimental results on mirror nuclei in the *sd* and *fp* shells are presented. Their respective Mirror Energy Difference (MED) diagrams are interpreted by means of large-scale shell-model calculations. A unique way of extracting effective charges from isospin symmetry studies is also discussed.

PACS. 23.20.Lv γ transitions and level energies – 21.10.Sf Coulomb energies – 21.60.Cs Shell model – 29.30.Kv X- and γ-ray spectroscopy

The isospin T is a good quantum number under the fundamental assumptions of charge symmetry and charge independence of the strong force, which imply that the proton and neutron can be viewed as two different states of the same particle, the nucleon [1]. However, the electromagnetic interaction between protons obviously breaks this symmetry. These effects can be studied in mirror nuclei, which are pairs of nuclei where the number of protons and neutrons are interchanged.

In this contribution we present novel results on mirror nuclei in the *sd* and *fp* shells, namely the $T_Z = \pm 1/2$ $A = 35$ [2], $A = 51$ [3,4], and $A = 61$ [5] mirror nuclei. The interpretation of the experimentally obtained Mirror Energy Difference (MED) diagrams in these systems goes beyond the traditional picture.

The $A = 35$ mirror nuclei were populated in an experiment at the Legnaro National Laboratory (LNL), where the heavy-ion fusion-evaporation reaction ^{24}Mg + ^{40}Ca was studied at a beam energy of 60 MeV [6]. As oxygen was present in the ^{40}Ca target the reaction ^{24}Mg + ^{16}O produced the $A = 35$ mirror nuclei ^{35}Ar and ^{35}Cl, via the evaporation of one α-particle and one neutron and one α-particle and one proton, respectively. The γ-rays were detected with the GASP array [7] in its standard configuration with 40 Ge detectors. For the detection of light, charged particles, the 4π charged-particle detector ISIS [8] was used. The NeutronRing replaced six of the 80 BGO elements at the most forward angles.

As expected, the resulting level energies of the $A = 35$ mirror nuclei displayed in fig. 1 are very similar. However, there are two obvious differences. The first concerns the γ-ray energies of the topmost $13/2^- \rightarrow 11/2^-$ transitions, which differ by as much as 300 keV. This difference

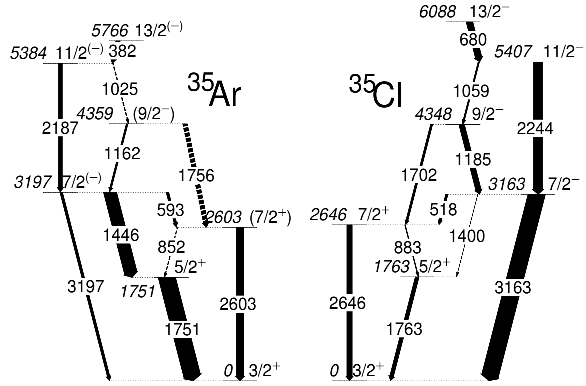

Fig. 1. Experimentally obtained level schemes for the $A = 35$ mirror nuclei. See text for details.

translates directly into a dramatic decrease of the MED at $J^\pi = 13/2^-$, which is shown in fig. 2. To understand the origin of the very large $13/2^-$ MED it is useful to follow the procedure outlined in ref. [9] and expand the Coulomb part of the MED in a Coulomb monopole component (Cm) and a Coulomb multipole component (CM). The CM component represents the effect of breaking and aligning pairs of protons and is expected to play a minor role for the $13/2^-$ states. However, the effect can be seen in the gradual decrease in the MED values between the $3/2^+$ and $7/2^+$ states and between the $7/2^-$ and $11/2^-$ states. In both cases this is the result when a pair of $1d_{3/2}$ protons (neutrons) aligning in ^{35}Ar (^{35}Cl). The Cm term can be expanded in several components. Here the focus is on one of them, namely the hitherto often overlooked electromagnetic spin-orbit component (Cls). Cls is a single-particle contribution and its effect is proportional to differences in the *differences* of neutron and proton orbital occupancies.

[a] Conference presenter. *Present address*: School of Technology and Society, Malmö University, SE-205 06 Malmö, Sweden; e-mail: `jorgen.ekman@nuclear.lu.se`

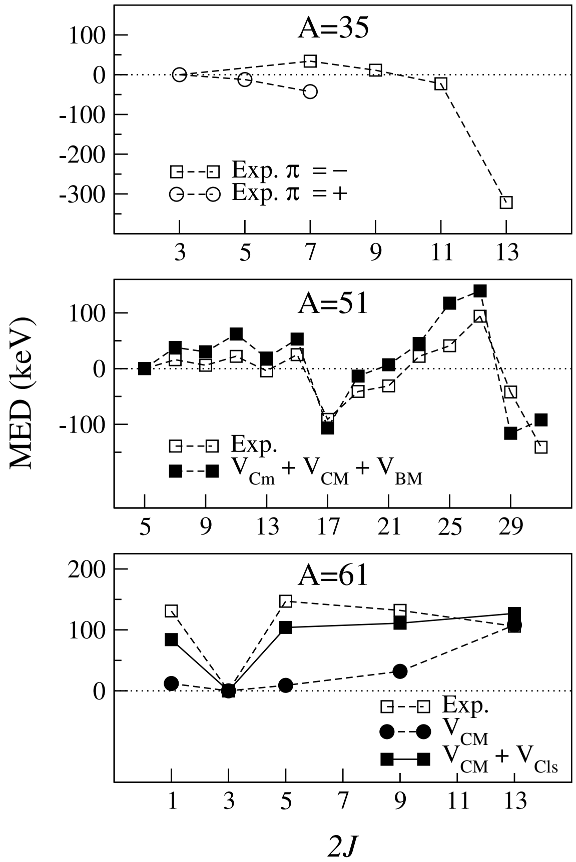

Fig. 2. Experimental and calculated MED values for the $A = 35$, $A = 51$, and $A = 61$ mirror nuclei.

It can be written as [10]

$$C_{ls} = (g_s - g_l)\frac{1}{2m^2_{\text{nucleon}}c^2}\left\langle \frac{1}{r}\frac{\mathrm{d}V_C(r)}{\mathrm{d}r}\right\rangle \langle \boldsymbol{l}\cdot\boldsymbol{s}\rangle\,, \qquad (1)$$

where g_s and g_l are the free gyromagnetic factors. For the negative-parity states in the upper *sd* shell the Cls term becomes significant. This is principally because the negative-parity states involve excitations from an orbital with $j = l - s$ to one with $j = l + s$. Specifically, there is a gain of some 100 keV for the $1f_{7/2}$ proton orbit with respect to the neutron orbit, and the $1d_{3/2}$ orbit loses almost as much. Shell-model calculations indicate that the $13/2^-$ states are the only states where the dominant configurations are based on $1f_{7/2}$ to $1d_{3/2}$ single-particle excitations. Thus the Cls term is expected to contribute with roughly half of the observed MED value of the $13/2^-$ states. To account for the remaining 150 keV other Coulomb monopole terms have to be considered [9,2].

The second remarkable difference comes from the decay pattern of the $7/2^-$ states. In ^{35}Ar the 1446 keV $E1$ branch clearly dominates the 3197 keV $M2$ decay, while the corresponding 1400 keV $E1$ decay is essentially absent in ^{35}Cl. The state decays directly to the ground state through the strong 3163 keV $M2$ transition. The effect is truly striking and has never been observed before in mirror studies. The dramatic difference in decay patterns of the $7/2^-$ states in the $A = 35$ mirror pair can also be seen when calculating the relevant transition probabilities. Using the known lifetime $\tau = 45.3(6)$ ps [11,12] of the $7/2^-$ state in ^{35}Cl, and the relative intensities of transitions [2] we obtain $B(M2; 7/2^- \to 3/2^+) = 0.25$ W.u. and $B(E1; 7/2^- \to 5/2^+) = 2\cdot 10^{-8}$ W.u. Assuming identical $B(M2)$'s in both members of the mirror system it follows that $B(E1; 7/2^- \to 5/2^+) = 3\cdot 10^{-5}$ W.u. for ^{35}Ar, which is three orders of magnitude larger than in ^{35}Cl. This huge difference in the $B(E1)$ values could in principle be explained by a cancellation of the $E1$ matrix elements due to isospin mixing. The amount of isospin mixing must then exceed five percent, which is much more than expected. However, there is no obvious reason for the assumption of identical $B(M2)$ values. In fact, assuming identical $B(E1)$ values is an even stronger criterion from isospin symmetry arguments [1]. However, this leads to $B(M2)$ values that differ with three orders of magnitude. Future investigations will hopefully pin down the driving mechanism responsible for the very asymmetric decay patterns of the $7/2^-$ states.

The $A = 51$ results are based on two different data sets. The first set is based on two Gammasphere experiments performed at the Argonne National Laboratory (1999) and at the Lawrence Berkeley National Laboratory (2001) [4,13]. Both experiments employed the fusion-evaporation reaction ^{32}S + ^{28}Si at 130 MeV beam energy. The γ-rays were detected in the Gammasphere array [14], which at the time comprised 78 Ge-detectors. For the detection of light, charged particles the 4π CsI-array Microball [15] was used. The Neutron Shell [16] replaced the five most forward rings of Gammasphere to enable the detection of evaporated neutrons. The reaction leads to the $A = 51$ mirror nuclei ^{51}Fe and ^{51}Mn following the evaporation of two α-particles and one neutron, and two α-particles and one proton, respectively. The second data set is based on an experiment aiming at measuring the lifetimes of the $27/2^-$ analogue states in the $A = 51$ mirror nuclei by means of the recoil distance Doppler shift technique. The experiment was performed at LNL using the reaction ^{32}S + ^{24}Mg with a beam energy of 95 MeV [3]. The enriched ^{24}Mg target was mounted inside the Cologne plunger device [17] and data were taken at 21 target-stopper distances ranging from electric contact to 4.0 mm.

From the Gammasphere data it was possible to identify some fifty core excited states in the $T_Z = +1/2$ nucleus ^{51}Mn [18]. Despite the much lower experimental cross section three (one tentative) previously unknown core-excited states were also identified in the $T_Z = -1/2$ mirror partner ^{51}Fe [4]. The obtained experimental level schemes (only the relevant part for ^{51}Mn) are shown in fig. 3 and the experimentally obtained MED diagram is shown in fig. 2 as open squares. The data up to spin $J = 27/2$ represent previously known experimental data [19,20], whereas the data points for $J = 29/2$ and $J = 31/2$ represent the new information arising from the yrast core excited states. As seen in fig. 2 the MED decreases rapidly from the fully aligned $J = 27/2$ states, which are based on a single $1f_{7/2}$ configuration ($\sim 70\%$), to the core excited states.

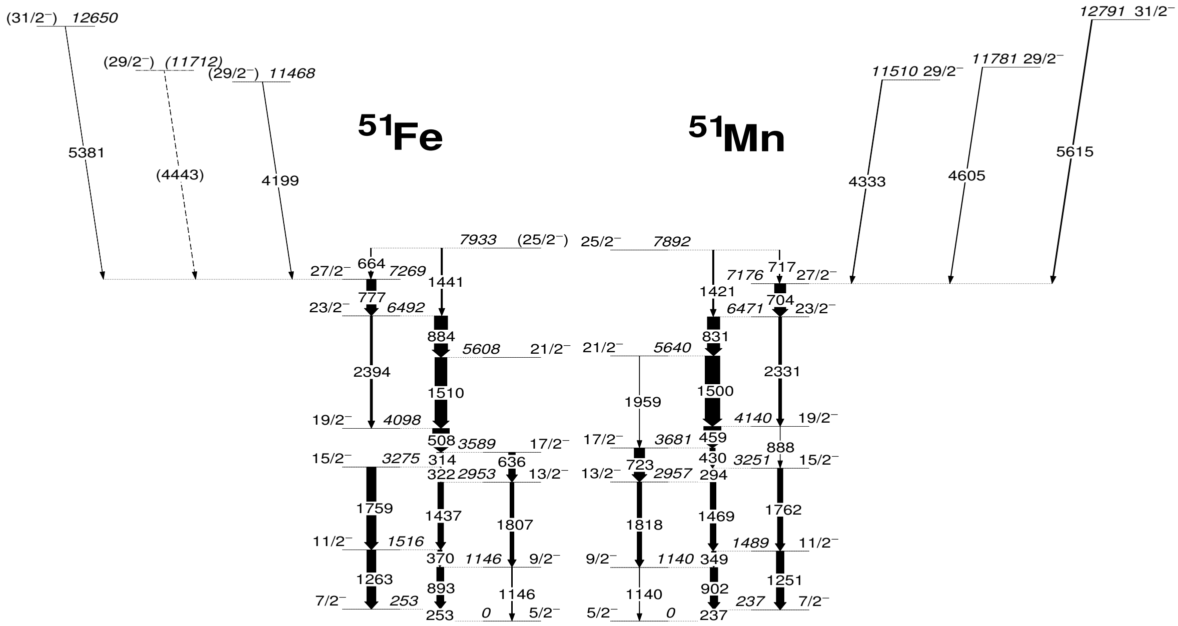

Fig. 3. Experimentally obtained level schemes for the $A = 51$ mirror nuclei. See text for details.

To interpret the experimental MED diagram large-scale shell-model calculations were performed using the shell-model code ANTOINE [21,22]. The calculations were performed using the KB3G with Coulomb interaction [23] in the full fp space containing the $1f_{7/2}$ orbit below and the $2p_{3/2}$, $1f_{5/2}$, and $2p_{1/2}$ orbits above the $N = Z = 28$ shell closures. The configuration space was truncated, *i.e.*, five particle excitations from the $1f_{7/2}$ shell to the upper fp shell were allowed. This was found to provide virtually identical results compared to calculations in the fp space without truncations on yrast states in $1f_{7/2}$ nuclei [23]. To account for the Coulomb interaction the proton two-body matrix elements were constructed by adding harmonic oscillator Coulomb matrix elements to the plain two-body matrix elements of the KB3G interaction. The calculations of MED values follow a procedure suggested and discussed in detail in ref. [9]. The results are included in fig. 2 as filled squares. Although the agreement for the yrast core excited states is not perfect it was found that the inclusion of the Coulomb monopole term is crucial for explaining the observed MED values.

The lifetimes of the yrast $27/2^-$ states in the $A = 51$ mirror nuclei was deduced from the LNL experiment. The resulting lifetimes are $\tau \sim 101$ ps and $\tau \sim 70$ ps for ^{51}Mn and ^{51}Fe, respectively [3]. To study the consequences of the lifetime results on polarization and effective charges large-scale shell-model calculations were performed using the shell-model code ANTOINE with the same model space and truncations as described above. Three different interactions were used in the analysis: The standard KB3G interaction without any Coulomb interaction, with theoretical harmonic-oscillator Coulomb matrix elements (Coulomb HO), and with the $1f_{7/2}$ Coulomb matrix elements replaced with the experimental values from the $A = 42$ mirror pair (Coulomb A42). The effective proton and neutron charges used in the calculations are expanded in terms of isoscalar $e^{(0)}_{\rm pol}$ and isovector $e^{(1)}_{\rm pol}$ polarization charges according to

$$\varepsilon_p = 1 + e^{(0)}_{\rm pol} - e^{(1)}_{\rm pol}\,; \qquad \varepsilon_n = e^{(0)}_{\rm pol} + e^{(1)}_{\rm pol}\,, \qquad (2)$$

To obtain agreement between experimental and theoretical $B(E2)$ values $e^{(0)}_{\rm pol} \sim 0.47$ and $e^{(1)}_{\rm pol} \sim 0.32$ must be used, almost independent of the interaction. This converts into effective proton and neutron charges of ~ 1.15 and ~ 0.80, respectively. Interestingly, this is very close to the predicted values in ref. [24] in the case of $N \sim Z$ nuclei. It was also investigated how the harmonic-oscillator parameter, b_0, which determines the radii of the wave functions, influences the polarization charges. As seen in fig. 4 the isoscalar polarization charge is affected the most when changing the b_0 parameter.

The $A = 61$ experiment was conducted at the Holifield Radioactive Ion Beam Facility (HRIBF) at Oak Ridge National Laboratory as described in detail in ref. [5]. In fusion-evaporation reactions of a ^{40}Ca beam at 104 MeV, impinging on a ^{24}Mg target foil, the mirror nuclei ^{61}Ga and ^{61}Zn nuclei were produced via the evaporation of one proton and two neutrons and two protons and one neutron, respectively. The Ge detector array CLARION [25] was used to detect the γ radiation at the target position. After the particle evaporation and prompt γ-decay processes the reaction products are recoiling from the thin target into the Recoil Mass Spectrometer [25] before finally being stopped in an Ionization Chamber.

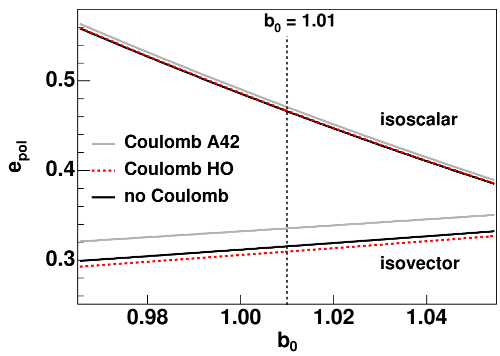

Fig. 4. Polarization charges, necessary to reproduce the $B(E2; 27/2^- \rightarrow 23/2^-)$ values in the $A = 51$ mirror nuclei, as a function of b_0 for three different shell-model calculations.

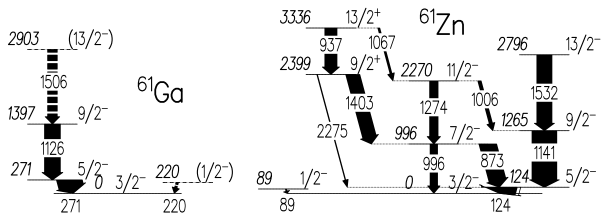

Fig. 5. Experimentally obtained level schemes for the $A = 61$ mirror nuclei. See text for details.

Four excited states in the $T_Z = -1/2$ nucleus ^{61}Ga were identified and are shown in fig. 5. When comparing with the relevant part of the ^{61}Zn level scheme, MED values represented by open squares in fig. 2 are obtained. Predictions from large-scale shell-model calculations using the shell-model code ANTOINE are included in fig. 2. The calculations were performed in the same model space as before, but this time the configuration space was truncated to allow for three particle excitations from the $1f_{7/2}$ shell into the upper fp shell. The calculations were performed using the GXPF1 [26,27] with Coulomb interaction. In the first calculation the standard GXPF1 single-particle energies were used for both protons and neutrons, to estimate the Coulomb multipole component. The result is shown as filled circles in fig. 2. It is seen that the correct sign of the MED values is reproduced, although the calculated MED values are typically 50 to 100 keV smaller than the experimental values. These discrepancies may be the result of Coulomb monopole effects discussed above, and especially the Cls component is expected to be important since excitations from the $2p_{3/2}$ orbit to the $1f_{5/2}$ and $2p_{1/2}$ orbits are present in the formation of the observed states. The result from a calculation where the single-particle energies have been modified according to eq. (1) is shown in fig. 2 as filled squares. It is seen that the agreement with the observed MED values has improved considerably. Last but not least it is intriguing to take a closer look at the level schemes in fig. 5. There is no apparent hint for the $9/2^+ \rightarrow 7/2^- \rightarrow 5/2^-$ (1403–873 keV in ^{61}Zn) or the $9/2^+ \rightarrow 7/2^- \rightarrow 3/2^-$ (1403–996 keV in ^{61}Zn) sequence in ^{61}Ga in the present data set, even though the branch through the 2399 keV $9/2^+$ state in ^{61}Zn has about the same intensity as the $13/2^- \rightarrow 9/2^- \rightarrow 5/2^-$ cascade. A possible explanation for the non-observed γ-rays decaying from a $9/2^+$ state in ^{61}Ga is a $1g_{9/2}$ proton decay from that level into the ground state of ^{60}Zn.

To summarize, experimental isospin symmetry studies have been extended to involve nuclei in the sd and upper fp shells. The importance of the hitherto overlooked electromagnetic spin-orbit effect has been shown. The strong asymmetry in the decay pattern of the $7/2^-$ states in the $A = 35$ mirror nuclei indicate the presence of isospin mixing and needs to be investigated further. Studies of the $A = 51$ mirror nuclei have revealed two interesting and novel features: i) mirror symmetry studies of core-excited states and ii) an unique way of extracting isoscalar and isovector polarization charges simultaniously.

The authors would like to thank all colleagues which partcipated in the experiments and the preparation of the manuscripts. A token of gratitude also goes to the accelerator crews at the various laboratories for their supreme effort in making the experiments succesful. This research was supported in part by the Swedish Science Council.

References

1. D.H. Wilkinson, *Isospin in Nuclear Physics* (North-Holland Publishing Company, Amsterdam, 1969).
2. J. Ekman *et al.*, Phys. Rev. Lett. **92**, 132502 (2004).
3. R. du Rietz *et al.*, Phys. Rev. Lett. **93**, 222501 (2004).
4. J. Ekman *et al.*, Phys. Rev. C **70**, 057305 (2004).
5. L.-L. Andersson *et al.*, Phys. Rev. C **71**, 011303 (2005).
6. C. Andreoiu *et al.*, Eur. Phys. J. A **15**, 459 (2002).
7. C. Rossi Alvarez, Nucl. Phys. News, **3**, 3 (1993).
8. E. Farnea *et al.*, Nucl. Instrum. Methods Phys. Res. A **400**, 87 (1997).
9. A.P. Zuker *et al.*, Phys. Rev. Lett. **89**, 142502 (2002).
10. R.J. Blin-Stoyle, Chapt. 4 in [1].
11. P.M. Endt, C. Van Der Leun, Nucl. Phys. A **310**, 1 (1978).
12. P.M. Endt, Nucl. Phys. A **521**, 1 (1990); **633**, 1 (1998).
13. J. Ekman *et al.*, Phys. Rev. C **66**, 051301(R) (2002).
14. I.-Y. Lee, Nucl. Phys. A **520**, 641c (1990).
15. D.G. Sarantites *et al.*, Nucl. Instrum. Methods A **381**, 418 (1996).
16. D.G. Sarantites *et al.*, Nucl. Instrum. Methods A **530**, 473 (2004).
17. A. Dewald *et al.*, Nucl. Phys. A **545**, 822 (1992).
18. J. Ekman *et al.*, Phys. Rev. C **70**, 014306 (2004).
19. J. Ekman *et al.*, Eur. Phys. J. A **9**, 13 (2000).
20. M.A. Bentley *et al.*, Phys. Rev. C **62**, 051303(R) (2000).
21. E. Caurier, shell model code ANTOINE, IRES, Strasbourg 1989-2002.
22. E. Caurier, F. Nowacki, Acta Phys. Pol. **30**, 705 (1999).
23. A. Poves *et al.*, Nucl. Phys. A **694**, 157 (2001).
24. A. Bohr, B.R. Mottelson, *Nuclear Structure*, Vol. **2** (Benjamin Inc., New York, 1975) Chapt. 6.
25. C.J. Gross *et al.*, Nucl. Instrum. Methods A **450**, 12 (2000).
26. M. Honma, T. Otsuka, B.A. Brown, T. Mizusaki, Phys. Rev. C **69**, 034335 (2004).
27. M. Honma, T. Otsuka, B.A. Brown, T. Mizusaki, Phys. Rev. C **65**, 061301 (2002).